Chapter 4: Experimental Techniques for Radium Partitioning Measurements

4.1 INTRODUCTION

The partitioning of radium into a major crustal constituent such as feldspar has important implications for deciphering the evolution and transport histories of young magmas, yet no experimental radium partitioning data exist for any mineral. This chapter discusses experimental and analytical approaches used to overcome the technical and safety challenges inherent to investigating partitioning behavior of the geologically short-lived radioactive isotope ^{226}Ra, which has a half-life of 1600 years and thus is over a million times more radioactive than the most abundant uranium isotope, ^{238}U (Figure 4.1). Here I outline the rationales for selection of the system composition, preparation of starting materials, and analytical method. Procedures used for handling the materials are detailed, as well as the design of a flow line to remove radioactive ^{222}Rn from gas exiting the furnace during experiments. Also described are post-experiment furnace contamination measurements and their implications for greater understanding of radium volatility. Experimental partitioning data for radium are discussed in chapter 5.

4.1.1 Crystal Chemical Model Prediction of Radium Partitioning in CMAS

The difficulty of experimentally determining Ra partitioning behavior has forced past workers to use Ba as a proxy, either by assuming barium partitioning behavior to be a perfect analogue (e.g., Condomines et al., 1995; Schaefer et al., 1993; Volpe and Hammond, 1991) or by extrapolating D_{Ra} from lattice strain models of partitioning.

Blundy and Wood (1994) demonstrated that cation partitioning behavior is often strongly and systematically dependent on ionic radius and resulting degree of fit or misfit into particular lattice sites. The difference between Ba, 1.42 Å in VIII-coordination (Shannon, 1976) and Ra (1.48 Å) leads to significantly predictions of Ra partition coefficients considerably lower than Ba. Accounting for this difference has notable implications for understanding the timescales of any magmatic process occurring within 8000 years, or five half-lives of ^{226}Ra. Failing to recognize the greater incompatibility of Ra relative to Ba in magmatic systems experiencing plagioclase crystallization produces an apparent crystallization age older than that of the actual event (Condomines et al., 2003). Cooper et al. (2001) showed the significance of this effect in the case of the 1955 Kilauea east rift plagioclases, which likely crystallized near the same time as the augite phenocryst population in this system, yet a ^{226}Ra-^{230}Th mineral isochron model assuming D_{Ra}/D_{Ba} = 1 would suggest the plagioclase crystallized 8000 years earlier. Given the demonstrated age uncertainties that these different estimates of D_{Ra} can imply in such systems, experimental determination of D_{Ra} would provide an important test of lattice strain model predictions for radium partitioning.

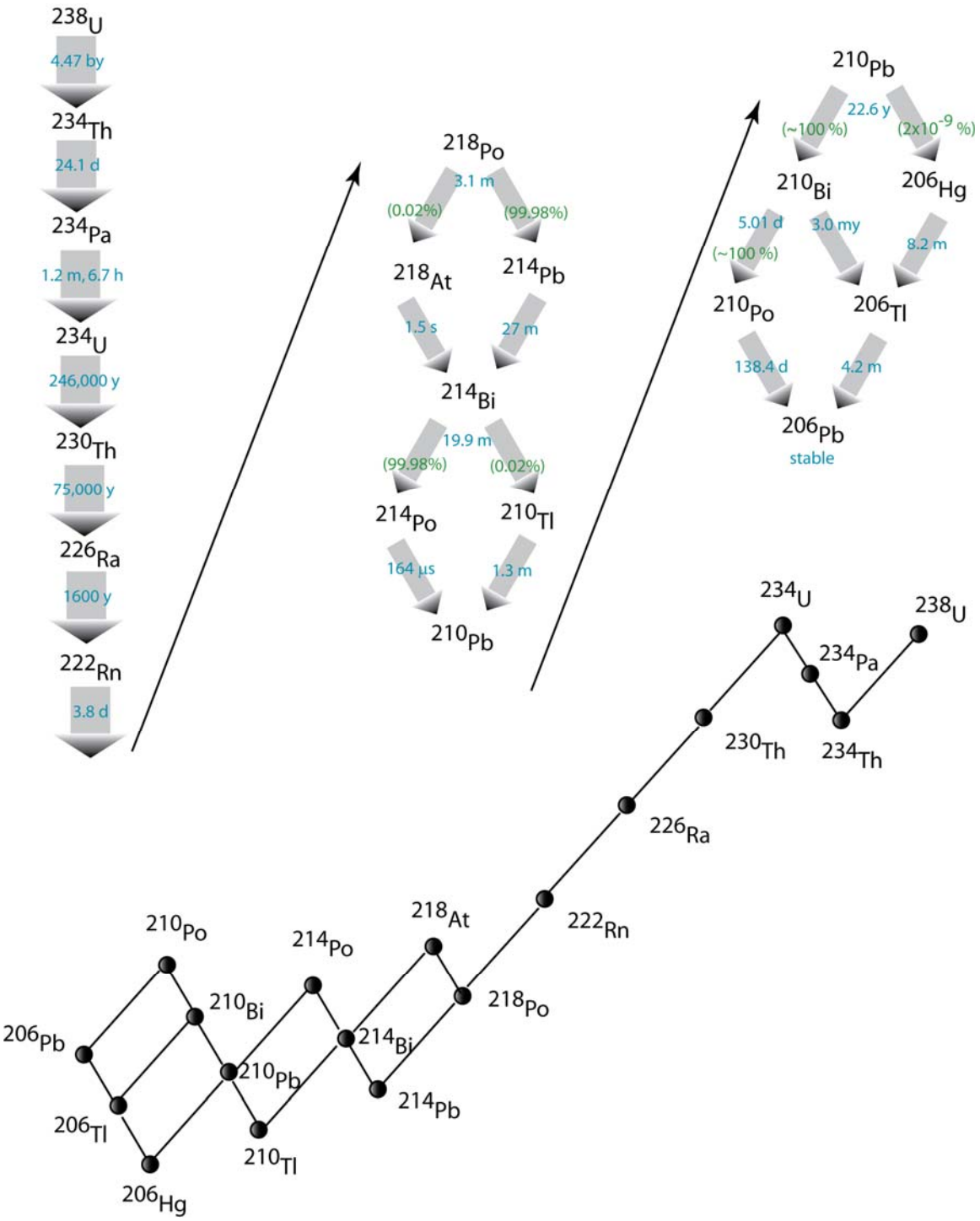

Figure 4.1. ^{238}U decay series ending in stable ^{206}Pb, with half-lives shown in light blue and % of daughter products produced (when several are possible) shown in green. Adapted from Parrington et al. (1996).

4.1.2 Analytical Method Considerations

Experimentally determined partition coefficients for radioactive elements such as U and Th have been measured by a range of analytical techniques including alpha and fission track radiography, proton-induced X-ray emission, laser ablation inductively coupled plasma mass spectroscopy (LA-ICP-MS), and secondary ion mass spectrometry (SIMS) (for a review, see Blundy and Wood, 2003a). Estimates of ^{226}Ra bulk and mineral/glass partition coefficients in natural samples may also be made by separating minerals from coexisting groundmass, digesting the samples, and measuring trace amounts of radioactive elements by isotope dilution thermal ionization mass spectrometry (TIMS) (e.g., Cooper et al., 2003; Cooper and Reid, 2003; Cooper et al., 2001; Rogers et al., 2004; Turner et al., 2003; Volpe and Hammond, 1991). Apparent D_{Ra} have also been obtained for leucite phenocrysts and groundmass by high resolution γ-spectrometry (Voltaggio et al., 2004). Such analyses can require tens to hundreds of grams of material (Condomines et al., 1995; Simpson and Grun, 1998). ^{226}Ra content determination for mineral and whole rock separates by ^{222}Rn emanometry also requires sample materials on the order of a gram (Schaefer et al., 1993).

Although destructive analytical techniques such as TIMS can detect very low amounts of ^{226}Ra (fg/g) in materials, *in situ* analysis was deemed a more suitable approach for accurately measuring radium in experimental run products of this study, given that the modest amount (<5 mg) of crystallized mineral material produced during an experiment would be difficult to cleanly separate from the coexisting glass phase and the extraordinary sensitivity of the measurement of very small partition coefficients to such contamination. The ~2.5 μCi of ^{226}Ra stock available to us made determining

plagioclase/melt partition coefficients by both alpha track radiography and SIMS potentially practicable.

4.1.2.1 Alpha Track Radiography Feasibility Tests

Alpha track radiography has the advantage of allowing *in situ* analysis of experimental samples, which relies neither on the cleanliness of natural material separates nor on the assumptions needed to derive a liquid composition from a groundmass or whole rock analysis. However, alpha track counting must be restricted to regions at least some critical distance from phase boundaries, depending on the alpha particle energies, to ensure that tracks collected at the sample surface did not originate at depth from a neighboring phase (LaTourrette, 1993).

As many radioactive elements of geologic interest belong to complicated decay chains (such as shown in Figure 4.1), there always exists a degree of uncertainty as to which tracks are produced by the decay of a particular element of interest. If one knows the abundances of each radioactive element in a sample, the track population corresponding to each can be calculated and accounted for when measuring a partition coefficient. The quantity of radium available for this study was obtained from Isotope Products in July of 1991, at which time the activity ratio of $^{210}Pb/^{226}Ra$ was reported as 4.8 %.

Since our radium starting solution contained a modest population of ^{226}Ra daughter product ingrowth, we needed to determine if those daughters would volatilize and depart the sample over the course of a controlled cooling experiment, which would

provide a clean initial condition for counting tracks produced by ^{226}Ra and a known quantity of daughter products at any point after the experiment. Several reconnaissance runs were performed to approximate the volatility of the longest-lived ^{226}Ra daughter nuclides ^{210}Pb ($t_{1/2}$ = 22.6 years) and ^{210}Bi ($t_{1/2}$ = 5 days) using an aliquot of CMAS1-1 composition material spiked with 2500 ppm Pb and 2500 ppm Bi. Volatility was not assessed for ^{210}Po, since Po lacks a stable isotope. Run products were analyzed on a JEOL 733 electron microprobe at Caltech; PbS and bismuth metal served as standards and beam conditions were 20 keV and 30 nA. Counting times were 30 s on the peaks and 15 s for background positions.

Compared to a 15 min glass fuse within a sealed 3 mm diameter platinum capsule (run 1-1-8), glass from an 86 hour open-furnace wire-loop dynamic crystallization experiment (run 1-1-7) contained no lead and 25 % of the initial bismuth. A 48 hr crystallization experiment (run 1-1-10) in an open graphite capsule under C/CO atmospheric conditions lost 90 % Pb and 45 % Bi, though measurement uncertainties (standard error of the mean) were somewhat large at 20 % and 35 % of the average glass totals for each element, respectively. Ideally, a quenched sample at the end of an experiment would have no significant population of alpha emitters except for ^{226}Ra so that all alpha tracks measured on film from the sample might be attributed to that one isotope. These Pb and Bi experiments indicated variable degrees of volatilization that could complicate interpretation of the alpha track population densities of both anorthite and glass when using alpha track radiography to determine radium partitioning.

4.2 STARTING MATERIAL PREPARATION

Given the complications for alpha track radiography associated with incomplete volatilization of daughter products over the course of the favored dynamic crystallization thermal regime for anorthite growth, we chose to measure radium partitioning behavior by ion probe. Major and trace element composition of starting materials were then picked specifically to maximize the fraction of the mass 226 signal attributable to ^{226}Ra during SIMS analyses.

4.2.1. Composition Selection

Selecting the optimal starting material composition for radium partitioning experiments from seven CMAS compositions (as described in chapter 2) relied on several factors. To maximize the amount of Ra available for detection in the anorthite crystals, one might choose CMAS2-7, the most magnesian composition. As a divalent cation with ionic radius of 1.42 Å in VIII-fold coordination, Ra^{2+} certainly enters the M-site of anorthite along with Ca, Sr, and Ba. Anorthite/melt partition coefficients presented in chapter 2 clearly demonstrate an increase in partitioning into the anorthite phase with increasing magnesium content of the coexisting CMAS liquid. However, the modest decrease in Ba D^{molar} values (0.21 ± 0.02 to 0.18 ± 0.2) from the CMAS2-7 to CMAS2-1 compositions suggests that this is a minor consideration, and if for other reasons the least magnesian composition (CMAS2-1) is preferred we should still be able to determine the lowest expected D^{molar}_{Ra} in this suite of compositions.

The accuracy of SIMS analyses can be compromised by the presence of ion clusters in the mass range of the cation of interest, especially for abundances near the detection limit of the instrument. The extent of this effect at mass 226 is unknown, so potential clustering of ions was estimated using the Excel macro "ClusterCalc," supplied by Ian Hutcheon and written by Ross Williams (Analytical & Nuclear Chemistry Division, LLNL), which utilizes the programming of O. Eugster et al. (1985). Gold coating was avoided to prevent possible mass 226 interference from ion clusters of ^{197}Au and ^{29}Si, since nearly 5 % of silicon in the sample exists as ^{29}Si (Parrington et al., 1996). By considering a population of H, C, O, Mg, Si, Al, Ca, Sr, and Ba ions, a mass tolerance window of 1.5, and a maximum cluster charge of 1, the most likely mass 226 interferences would result from two-ion clusters of various Ba and Sr isotope combinations. To minimize this potential interference, the starting material was doped with ~100 ppm Ba and ~100 ppm Sr, a factor of 30 lower in the case of Ba than the amount used for the partitioning studies of chapter 2. Less likely three-ion clusters might involve addition of hydrogen to Ba-Sr clusters. Magnesium isotopes featured prominently in a number of possible four ion clusters and thus the least magnesium rich of our CMAS2 compositions, 2-1, was selected for use in our radium partitioning study.

No standard exists for radium, so radium content must be determined by comparing the measured abundance of ions detected at mass 226 for a sample with known non-zero radium concentration to an otherwise identical sample lacking radium, following the method of Brenan et al. (1995). Doping a 150 mg aliquot of starting material with approximately 1 μCi of ^{226}Ra would produce a mixture with roughly 1 ppm RaO. If the anorthite-melt radium partition coefficient were ~0.1, the SIMS would need

to accurately detect concentrations on the order of 100 ppb Ra in the anorthite phase in order to determine a partition coefficient. Here we document the procedure for making such a standard; ion probe sensitivity tests showing that this abundance is sufficient for successful measurements follow in the next chapter.

4.2.2 ^{226}Ra Solution Preparation

Source material for radium in this experiment was a reported 1 μCi of ^{226}Ra in 0.1 mL of 1 M HNO_3 from Isotope Products Laboratories. Daughter products had been separated from the ^{226}Ra in December 1989 resulting in a reported a_{Pb}/a_{Ra} of ~4.8 % as of July 1, 1991. The seal on the glass vial containing the radium solution was broken at some point prior to March 2005 and the solution had completely dried, likely leaving a $Ra(NO_3)_2$ salt residue. The remaining radium salt was resolubilized in 1 mL 5 M nitric acid by shaking vigorously under a heat lamp. The solution was transferred to a sterile 2 mL polypropylene NALGENE cryogenic vial with a 1 mm thick wall.

Gamma spectra of the solution in the plastic vial were collected in the Safety Office of the California Institute of Technology using a GEM 30P high purity germanium coaxial detector and ORTEC DSPEC jr digital gamma-ray spectrometer. Data were processed with GammaVision-32 gamma ray spectrum analysis software. Gamma rays from the vial were counted over a 1 hour period to obtain a spectrum. Approximately 94.45 % of ^{226}Ra α-decays go directly to the ^{222}Rn ground state, but the remaining 5.55 % of the decays go to the 2+ excited state, which returns to the ground state by release of a 186.2 keV gamma ray.[1] This 186 keV peak, the most intense of the ^{226}Ra

[1] Based on NNDC/BNL 5/1/2000 data compiled in the Idaho National Laboratory gamma-ray spectrum catalogue.

gamma ray energy spectrum, was compared to that detected from a 5 μCi standard ^{226}Ra source over an equal period of time. The 5 μCi standard is uncertified and therefore has a presumed uncertainty of 15 %. The spectrometer measured 2.6 ± 0.4 μCi of ^{226}Ra from the vial.

4.2.3 ^{226}Ra-Spiked Starting Material Preparation

Starting material consisted of 0.5 g of CMAS2-1 composition powder spiked with 150 ppm Ba and 100 ppm Sr according to the procedures described in chapter 2. A 150 mg aliquot of this material then was doped with ^{226}Ra by emptying the 1 mL contents of the polypropylene vial onto a Teflon watch glass and reducing the size of the solution drop under a heat lamp in a fume hood of the Caltech Isotope Lab. Four 1 mL washes of the vial using heated 5 M HNO_3 and vigorous shaking were added to the watch glass bead and subsequently reduced under heat until the remaining bead attained a diameter of ~0.8 cm. Gamma counting of the empty vial confirmed that no significant ^{226}Ra remained in the vial. The 150 mg of starting material was added to the reduced solution bead in a glove box in the same hood and mixed with a Teflon coated spatula. Several drops of 2 % polyvinyl alcohol aqueous solution were added to the mixture, which was formed into a large bead and transferred onto a circular mesh of platinum wire suspended from an alumina rod to be lowered into a vertical muffle furnace.

The bead exterior remained wet after an intended overnight drying period, so the bead was hung for two hours at the top of Deltech furnace muffle tube, where it dried at ~220 °C under compressed air flow. It was then lowered into the hot spot of the furnace and the furnace temperature was raised to 1440 °C where the bead fused for three hours.

The fused material was air quenched by turning off the compressed air flow and removing the bead from the top of the furnace.

4.3 EXPERIMENTAL DESIGN

4.3.1 Furnace Setup for ^{226}Ra Experiments

The primary safety objective of conducting radium partitioning experiments for ion probe analysis is containment of the radioactive radium and daughter products that are emitted from the charge over the course of an experiment. ^{226}Ra decays by alpha particle emission to ^{222}Rn gas, which has a half-life of 3.8 days. Assuming that radium volatility is negligible at 1400 °C at atmospheric conditions, the challenge lies in trapping the radon released from the sample material during the fusing of the doped starting material and during the ~100 hour controlled cooling experiment. To accomplish this, a multi-step flow line was constructed with an activated charcoal trap to remove radon from the air exiting the furnace. Several other reservoirs were positioned before the radon trap to remove other daughter nuclides and any water or carbon dioxide from the flow stream that might reduce radon adsorption efficiency of the activated charcoal.

4.3.2 Activated Charcoal Selection and Preparation

The radon trap consisted of 3 mm diameter pellets of extruded activated carbon from NORIT Americas (product R-2030). Previous work comparing radon adsorption onto various activated charcoal brands showed that NORIT activated carbon performed best (Bocanegra and Hopke, 1988) among the products considered. A separate study

comparing six active carbons from Kuraray Chemicals reported the best adsorption performance by a carbon (referred to as "KAC-3") with an apparent density of 0.40 g/ml and specific surface area (N_2 BET) of 910 m^2/g (Nakayama et al., 1994). The physical properties of the NORIT R-2030 activated carbon used here with apparent density of 0.56 g/ml and 800 m^2/g surface area are more like those of the most absorbent Kuraray carbon than any other investigated by Nakayama and coworkers.

To enhance adsorption performance, several studies recommend heat treating activated carbon under vacuum prior to use to remove water (Johnson et al., 1998; Momyer, 1960; Nakayama et al., 1994). This step was clearly necessary, as water condensation was observed along the interior regions below the two glass stoppers of the glass apparatus when fresh carbon pellets directly from the NORIT container were heated while the apparatus was sealed off from the vacuum line. The activated charcoal glass reservoir was heated to >150 °C by wrapping the reservoir exterior with flexible electric heating tape and then placed under vacuum sustained by a roughing pump. The charcoal was heated under vacuum for a minimum of thirty minutes and then the chamber was sealed to keep the charcoal isolated from ambient atmospheric conditions until the experiment commenced shortly thereafter. For added insurance that material would not be sucked into the pump, a series of glass tube loops in a water–ice bath served to trap any particles or unwanted gases before they entered the pumping system (Figure 4.2).

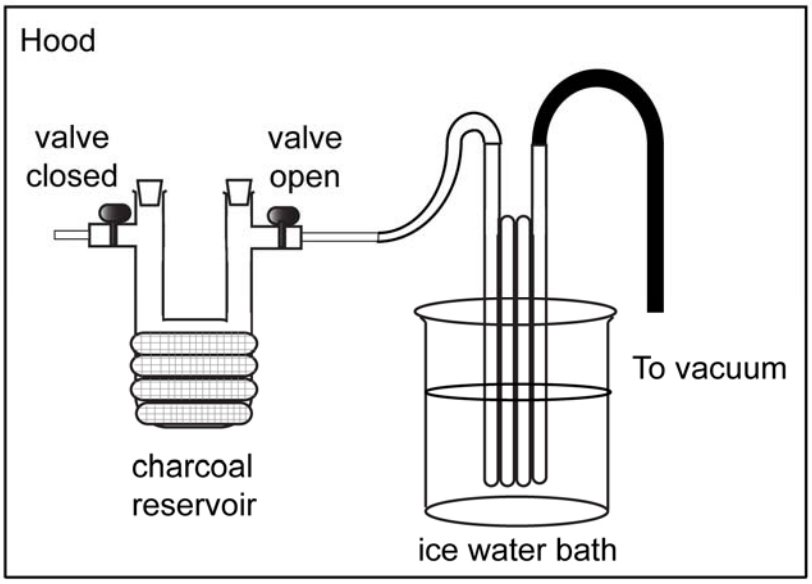

Figure 4.2. Flow line configuration for activated charcoal heating pre-treatment under vacuum prior to sample runs in furnace.

4.3.3 Flow Line Design

Gas flowing through the system consisted of Air Liquide Alphagaz1, an airlike synthetic nitrogen-oxygen mixture with 20 %–22 % O_2, <3 ppm H_2O, <1 ppm CO_2, and <2 ppm total hydrocarbons. Typical flow rate was approximately 75 cm^3/min. The gas entered the top of the furnace and exited the bottom, step (1) of Figure 4.3, after which it bubbled through a glass dispersion tube with a coarse (170-220 μm pore size) frit into 5 M HNO_3 solution (2) intended to remove any airborne lead, bismuth, or polonium daughter products produced from the charge (Bagnall, 1957). The gas then bubbled through a second frit into a saturated NaOH solution to remove CO_2 from the gas stream (3).

Passing through two liquid reservoirs added moisture to the gas, so two aspirator bottles of $CaSO_4$ (indicator Drierite) were constructed next to remove any H_2O from the gas flow, steps (4) and (5). As a final insurance step to remove any remaining CO_2, the gas proceeded through a second CO_2-removal step (6) consisting of an aspirator bottle filled with DeCarbite, a granular silica base coated with NaOH to provide a large surface area for CO_2 absorption. To keep the DeCarbite grains from sticking together, the product was interspersed with vermiculite as recommended by the manufacturer. The gas then flowed into the activated carbon chamber (7), which contained approximately 100 g of activated charcoal, in a water-ice bath contained by a 1.9 L capacity dewar flask.

Radon has a boiling temperature of −61.7 °C (CRC, 1993-1994), so preliminary tests of the flow line included a dry ice–ethanol bath (−97 °C). Trial runs with the dry ice–ethanol bath demonstrated that the activated charcoal chamber was efficiently trapping a relatively large volume of an unknown gas that might compete with radon for pore space within the charcoal pellets. Alphagaz1 is synthesized by mixing pure O_2 and N_2 gases rather than by directly purifying and compressing ambient air, but the Ar contents of Alphagaz1 are not routinely measured or reported in product literature so it remains a possible candidate. To mitigate this potential competition, a water-ice bath was chosen instead under the assumption that the 0 °C conditions still would be sufficiently cold to trap the relatively heavy radon gas within the chamber but not other more abundant, but more volatile, gas species. To test the efficiency of the flow line in removing H_2O and protect the charcoal reservoir from any back-streaming air moisture, a third Drierite step (8) was added after the charcoal chamber.

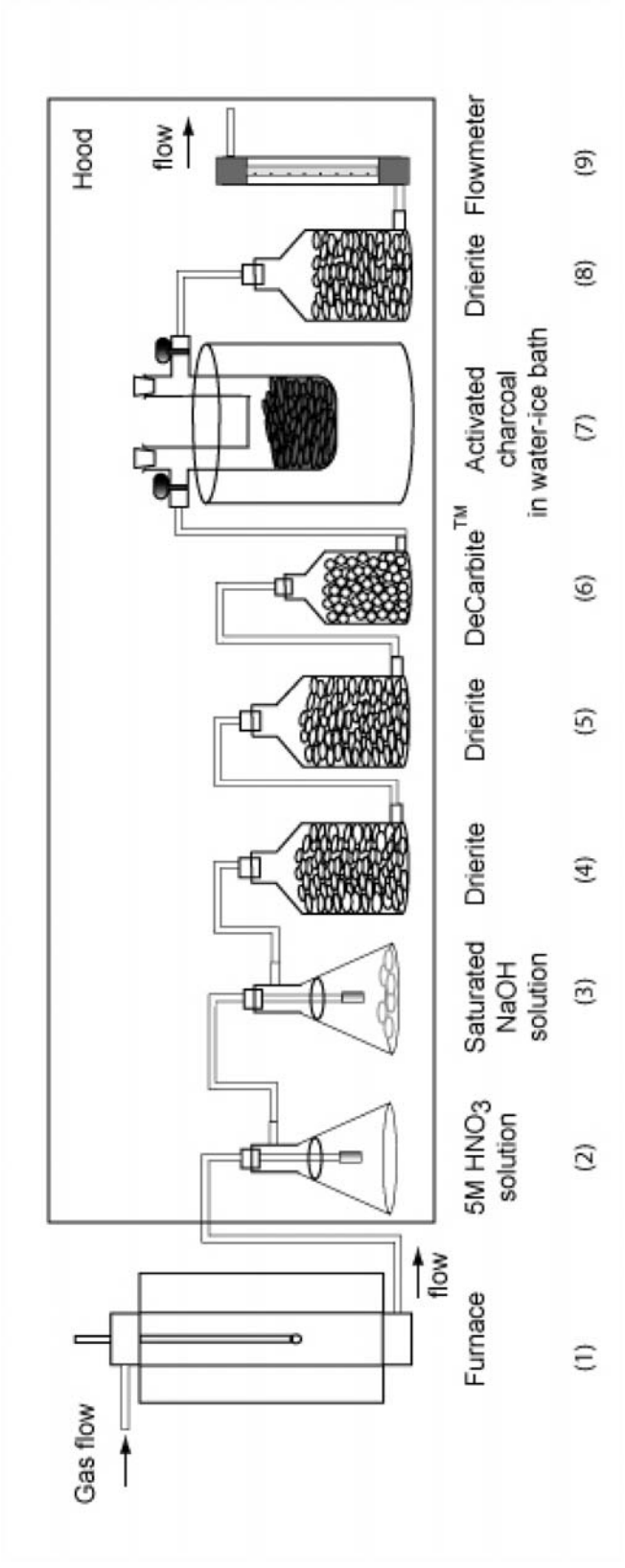

Figure 4.3. Flow line for ^{222}Rn removal from gas exiting furnace during experiments.

This drierite reservoir showed no visual indication of water absorption over the course of the experiments. Gas then passed through a flow meter out into the back of the hood (9).

After the experiment, the charcoal reservoir was sealed on both ends by closing the valves, removed from the flow line, transferred to a large plastic bag, and placed in a –10° C freezer for five months to ensure that nearly all of the trapped radon atoms would have decayed to non-gaseous daughter products. The charcoal was then removed from the freezer.

4.4 POST-EXPERIMENT FURNACE ANALYSIS

4.4.1 Activity Measurements of Sample Rod

Efforts to minimize system contamination assumed that ^{222}Rn gas would be flushed through the system by gas flow and collected in the charcoal cold trap, whereas ^{226}Ra volatilization would be negligible. Detailed, direct studies of radium volatility do not exist, though it is qualitatively described as being somewhat more volatile than barium (Bagnall, 1957; Bouissieres, 1958). To assess the extent and nature of possible contamination of furnace elements with Ra volatilized from the experimental charge, the ~47 cm alumina hanging rod was cut after the experiment into ten sections according to levels of activity measured by Geiger counter. To ensure that only ^{226}Ra would be producing any measured activity, this was performed three months after the experimental work. Sectioning occurred in a hood glove box of the Caltech Isotope Lab using a Dremel diamond wheel. The two ~13 cm ends of the alumina rod registered no discernable activity above background levels and were not subdivided. Activity was

concentrated in the middle 20 cm of the rod, which was sectioned into eight lengths. Rod sections were contained in reclosable low density polyethylene bags with wall thickness of 0.1 mm, and activity of each segment was measured using a Geiger counter and by γ-spectrometry.

Each bagged segment was placed on a surface 2.5 cm below a Ludlum in-window gas detector Geiger counter with the counter reading reported as an eyeball estimate of the range of counts detected while watching the counter for approximately a minute. Results are reported in Figure 4.4(d) and indicate that detected activity varies with position of the alumina rod in the furnace according to the thermal gradient. Activity rises above background levels between 700 °C and 800 °C, and Geiger counter readings suggest it peaks around 500 °C before decreasing to background levels at the top of the furnace.

The alumina rod had been used previously in C/CO buffered experiments, during which amounts of carbon were deposited on the rod that were qualitatively similar to the activity variations measured. This heterogeneous carbon surface may have also influenced ^{226}Ra deposition if the radium preferentially adsorbed onto carbon relative to alumina.

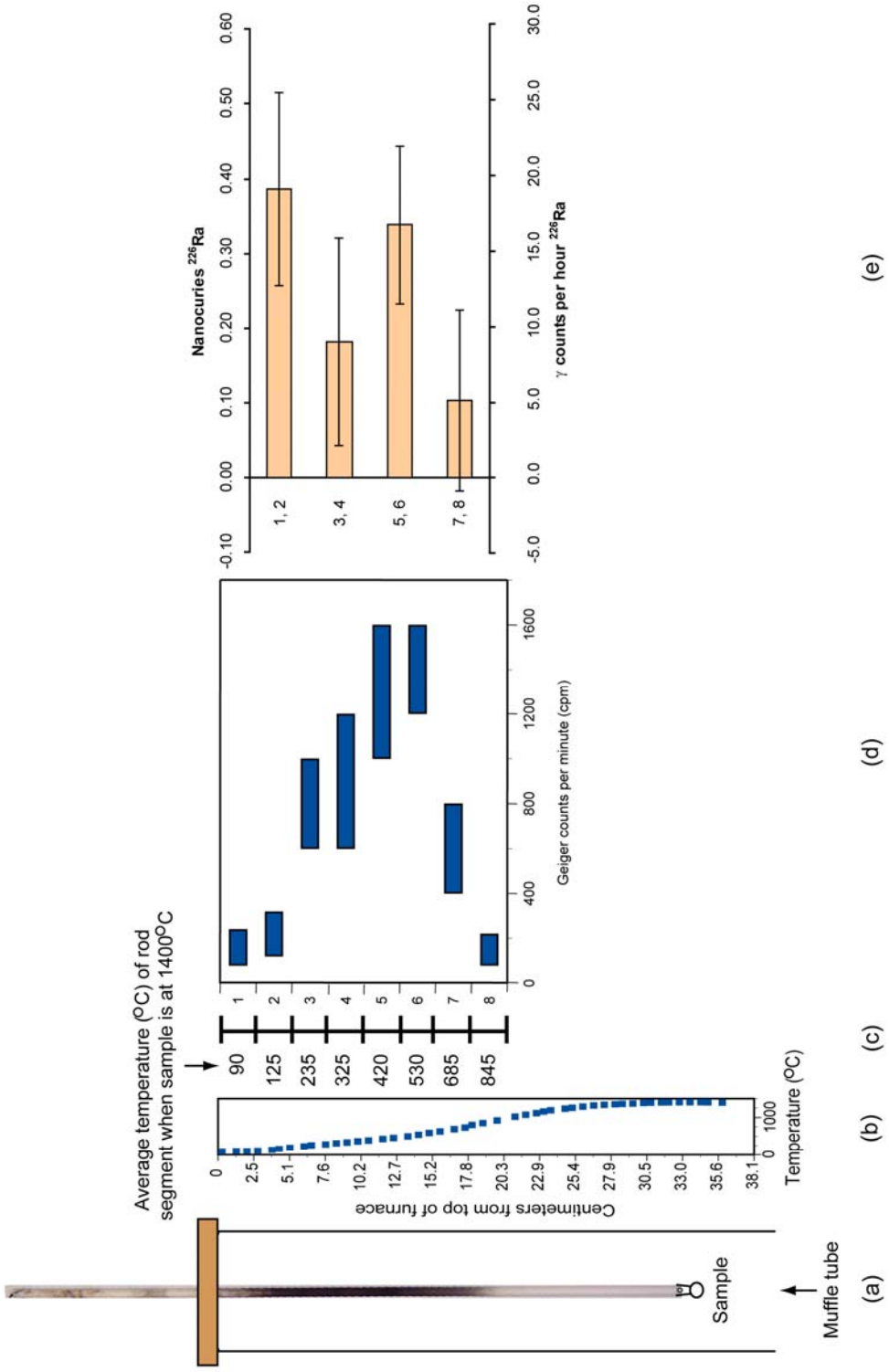

Figure 4.4. (a) Image of rod relative to muffle tube and sample in furnace, (b) thermal profile of furnace when sample location = 1400 °C, (c) average temperature of middle of each sectioned rod segment when sample is at 1400 °C, (d) rod segment activity measured by Geiger counter (counts per minute), (e) nCi ^{226}Ra and corresponding particle counts detected by γ-spectrometry for each pair of rod segments.

Geiger counters can only detect the intensity of ionizing radiation, not species identity, so γ spectra were collected to determine the activity source. The activity source concentrations on each rod segment were near detection limits of the spectrometer, so segments were paired and the four groups were each measured for 24 hours and their spectra compared to that of a 1.57 μCi ^{226}Ra standard and a 24 hour background spectrum. Each was positioned 10 cm from the detector, with the goal of being close enough to ensure detection yet not so close as to influence readings by the differing geometries of the rods and the source. Radium concentrations for each set of rod segment pairs is shown in Figure 4.4(e), with uncertainty calculated from the error associated with the background channel measurements immediately below and above the ^{226}Ra peak locations.

4.4.2 Radium Volatility

Although radium volatilization was anticipated to be essentially nonexistent, it occurred nonetheless. Assuming that the maximum activity recorded by Geiger counter represents 0.2 nCi of ^{226}Ra (from Figure 4.4(e)), application of an integrated rod deposition profile to the 4.75 cm diameter alumina muffle tube interior generates an estimated 8 nCi of total ^{226}Ra activity in the furnace after experimental work was complete. The furnace experienced two stages of potential ^{226}Ra exposure: the 3 hour fusing of the 2.5 μCi starting glass material and the 102 hour dynamic crystallization experiment CMAS2-1*-Ra with a sample activity of 0.5 μCi. Relative to the sample

^{226}Ra contents, Geiger and γ-spectrometry measurements indicate that ~1.5 % of the radium was lost over the course of the experiment.

Atomic mechanisms for radium volatilization from this CMAS composition are unknown. What radium left the sample did so at temperatures between ~1320 °C and 1440 °C and condensed primarily in the 200–700 °C range of the furnace. The furnace atmosphere was maintained with a very oxidizing gas flow containing ~20 % O_2, making it unlikely that radium would have been present as a monatomic species, though radium metal has a melting point of 700 °C, lower than that of any other alkaline earth nuclide except magnesium. No chemical data exists for RaO; however, the boiling temperatures of other group II oxides of the periodic table systematically decrease from ~3900 °C to ~2000 °C with increasing atomic number (CRC, 1993-1994). Whether RaO volatilizes at temperatures at or below those of the experimental conditions remains undetermined and would not be necessarily expected, given that radium is thought to have a number of electrochemical properties very similar to barium (e.g., Pauling electronegativity, which is 0.9 vs. 0.89, respectively (Allred, 1961; Pauling, 1960)) and thus might be expected to behave similarly. Strontium, by comparison, is notably more electronegative at 0.95 (Allred, 1961), consistent with the flattening trend of most periodic properties approaching the bottom of each group.

Experimental studies of major element species volatility and condensation within the solar nebula have shown that, under reducing atmospheric conditions, Mg and Si can evaporate from condensed phases (Davis et al., 1999; Richter et al., 1999). Electron microprobe point transects from the edges inward of glass beads heated to 1400 °C under

compressed air flow for 100 hours were analyzed, which verify that this evaporation did not occur under the oxidizing atmospheric conditions used for these studies.

Work on calcium by Hashimoto (1992) introduces another possibility for alkaline earth element volatilization: formation of gaseous $M(OH)_2$, where M represents an alkaline earth element. Experimental determination of the thermodynamic properties of hydroxide species involved in the reaction

$$CaO_{(s)} + H_2O_{(g)} \rightleftharpoons Ca(OH)_{2\,(g)} \qquad (4.1)$$

allowed Hashimoto to calculate various Ca species stabilities for a variety of temperature, fO_2, and log(H/O) conditions pertinent to models of the solar nebula. These conditions are admittedly quite different from that of our radium experiment furnace environment. The total gas pressure of the hydroxide experiments was a factor of 1000 lower than in the radium partitioning study here, and modeling in Hashimoto (1992) is restricted to log(H/O) above −2.8, whereas the maximum 3 ppm H_2O content of the Alphagaz1 used here would create a furnace log(H/O) = −4.8. Also, the log(fO_2) of this radium work is very oxidizing, close to 0, whereas Hashimoto models the log of partial oxygen pressures from approximately −5 to below −40. Nonetheless, the formation of gaseous alkaline earth hydroxides under the radium experiment conditions cannot be ruled out. At any given time, assuming constant rates of radium volatilization over the course of a controlled cooling experiment, the ratio of H_2O/Ra in the gas phase exceeds 10^7, which is an ample supply of water molecules. Hashimoto also found that in a relatively oxygen-poor environment [log(H/O) = 3.16] monatomic and oxide species were most abundant above 780 °C, whereas at log(H/O) = 1.6, $Ca(OH)_2$ was the dominant species up to ~1530 °C. These calculations suggest that $Ra(OH)_2$ could be considered a potentially stable

gaseous phase under the experimental conditions of our study, though no chemical data on this compound exist to support or eliminate this possibility.

While the gaseous species and volatility mechanism are uncertain, it remains a fact that activity measurements of the sectioned sample rod clearly indicate that a small but notable quantity of radium both volatilized and condensed within the furnace thermal gradient over the course of the experimental work. Future high-temperature experiments on Ra-bearing materials should be designed not only to capture Ra but also to ensure that all elements of the furnace that sit above ~200 °C in the thermal gradient are treated as radioactive byproducts.